Neutron-scattering study of methane bilayer and trilayer films on graphite

J. Z. Larese, M. Harada,* and L. Passell
Brookhaven National Laboratory, Upton, New York 11973

J. Krim
Department of Physics, Northeastern University, Boston, Massachusetts 02115

S. Satija
Department of Physics, University of Delaware, Newark, Delaware 19716
(Received 22 May 1987; revised manuscript received 21 October 1987)

The results of a neutron-diffraction study of the multilayer growth properties of methane on a graphite substrate are presented. The experiments, performed over an extended temperature range, follow the layering behavior from the submonolayer region to approximately three layers. The completed monolayer film is found to be overcompressed with respect to the bulk value. A stacking sequence and lattice parameter close to that of the bulk solid are found near three layers. The bilayer region, however, is characterized by a diffraction pattern which is not consistent with two layers in perfect registry with one another.

INTRODUCTION

The layer-by-layer growth of thin solid films on solid substrates poses problems of both fundamental and practical importance. Much attention has recently been directed towards understanding the underlying principles which govern how such a film attains macroscopic dimensions.[1] Theoretical studies aimed at understanding the microscopic mechanisms which are responsible for multilayer growth have focused on the relative strengths of the adsorbate (A) and substrate (S) interactions.[2-4] These studies suggest that for strong A-S interactions uniform layer-by-layer growth (wetting) occurs at $T=0$. Experimental studies find that for nonzero temperatures complete wetting occurs for only a limited range of relative A-S and A-A interaction strengths. Systems where the ratio of A-S to A-A interactions falls outside this region exhibit layer growth which is of the incompletely wet or Stranski-Krastanov type. It is this latter type of incomplete wetting that appears to be the typical mode of layer growth. Furthermore, in the limit of highly attractive substrates it has also been suggested that the initial adsorbed layers can have lattice constants which may be significantly different from those occurring in the bulk material. Experiments involving the wetting behavior of methane on graphite indicate that it falls slightly outside the complete wetting regime.[5]

The purpose of this study was to investigate by neutron diffraction how the first few layers of an adsorbed solid film develop and what effect this initial growth has on the wetting behavior. Overlayers of methane physisorbed on graphite were chosen because past experiments demonstrated that between four and six uniform solid layers could be deposited above 20 K,[5,6] suggesting that methane might serve quite well as a model system. Additionally, this work was stimulated by the recent detailed calculations of the thermodynamic and structural properties of monolayer, bilayer, and trilayer methane films by Phillips,[7,8] the results of which indicated that the first few layers of methane may have lattice constants which are more compressed than the bulk solid at the same temperature. Neutrons are ideally suited to probe this type of growth process because of their weak interaction with matter. This ensures that the signal from the diffracted neutrons will be characteristic of the entire multilayer and not just the outermost layer of the film.

MULTILAYER LINE SHAPES

Underlying our measurements is the question of how the scattered neutron intensity will change as a system proceeds from a single layer to a multilayer. This can be answered in a very intuitive way. First, consider the nature of reciprocal space for an infinite two dimensional (2D) solid. From elementary diffraction theory recall that in a 2D system reciprocal space is composed of a series of Bragg rods which are the direct result of the fact that only two Laue conditions (rather than three) must be satisfied. Similarly, the situation for three dimensions is also well known; reciprocal space being characterized by a set of Bragg points. Ideal 2D or 3D solids will have reciprocal lattices composed of rods (2D) or spots (3D) represented by delta functions; finite crystallite sizes will result in rods or spots of nonzero width. Consider what changes take place in this simple picture of reciprocal space when we have a system which now grows from a single layer towards a 3D structure. One can easily imagine that the Bragg rod characteristic of the 2D lattice becomes progressively modulated in such a way as to eventually produce Bragg spots representative of the growth in the third dimension (see Fig. 1). Although this very intuitive picture has some distinct shortcomings, it nonetheless provides the basic framework for the discussion which follows.

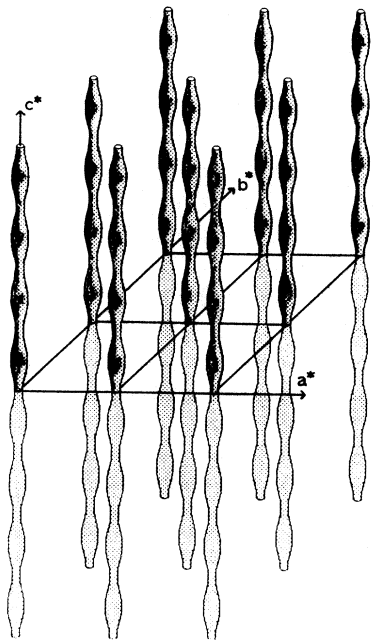

FIG. 1. A schematic representation of a portion of reciprocal space is shown for a spatially finite, bilayer structure.

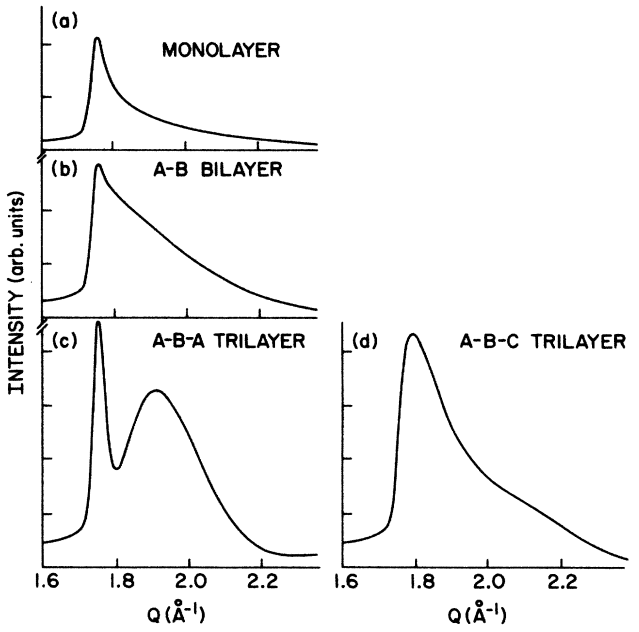

FIG. 2. Model line-shape calculations for a powder-averaged diffraction profile resulting from an *A-B* stacking sequence for (a) monolayer, (b) bilayer, (c) trilayer thick film. (d) illustrates the diffraction profile for an *A-B-C* trilayer. A triangular, commensurate, close-packed structure was used in each case. The in-plane lattice spacing was the same in all cases. The interplane distance was held fixed between all layers.

As previously mentioned, our concern here is an analysis of a neutron-diffraction study of the multilayer adsorption of deuterated methane (CD_4) on graphite. In order for these experiments to be performed with neutrons it is common knowledge that one needs a substrate which has a large surface-to-volume ratio. The substrate used for this experiment (vermicular graphite) has many, uniform, exposed basal planes with a random distribution of *c*-axis directions. This type of substrate necessitates a powder-averaging procedure which has been the topic of many previous works, the most recent being that of Stephens *et al.*[9] Here we deal specifically with the multilayer interference term $F(Q_z)$ referred to in the appendix of that work (Q_z is the *z* component of the wave vector **Q** with respect to a coordinate system fixed on a given crystallite). In order to calculate $F(Q_z)$, which describes the way in which the rod is modulated, one must first make some assumptions concerning the arrangement of the atoms or molecules within each layer of the film. The present discussion will consider only 2D layers of molecules characterized by triangular in-plane structures. The CD_4 molecules within the solid are assumed to be isotropically reorienting, which allows a spherically symmetric molecular form factor (as described by Press *et al.*[10] for bulk CD_4) to be used. This assumption should be quite good considering the temperature range in which the experiments were performed. It should be noted that the severe damping effect of the molecular form factor restricts the diffraction information to only the lowest index peak. The in-plane lattice of each layer is assumed to be commensurate with all other layers. Also the interplanar distance is kept uniform. These conditions are consistent with the theoretical findings of Phillips.[8] Calculations were carried out for both *A-B-A* and *A-B-C* stacking sequences. Figure 2 shows a typical profile for a monolayer, bilayer, and trilayer film calculated using the simple model outlined above. The line shapes were obtained by assuming that a powder-averaged Lorentzian profile (multiplied by a form factor for spherically disordered molecules) would be modified such that the modulation along the axis of the rod arises from the usual structure factor expression:

$$F_{hk}=\sum_j \{b_j \exp[-2\pi i(hx_j+ky_j+Q_z cz_j)]\} \ . \tag{1}$$

In these results *c* refers to the interplanar distance and Q_z is the component of **Q** normal to the layer plane. For monolayer films the *z* coordinate of the molecules does not enter explicitly into the problem. It is, however, this component which is directly responsible for the characteristic shape of the multilayer diffraction patterns. Restricting our attention to the first-order Bragg reflection and identical scatters, the following functional forms are readily obtained:

$$|F_{\{10\}}|^2=b^2[2-\cos(cQ_z)] \ , \tag{2}$$

$$|F_{\{10\}}|^2=b^2[3-2\cos(cQ_z)+2\cos(2cQ_z)] \ , \tag{3}$$

$$|F_{\{10\}}|^2=b^2[3-2\cos(cQ_z)-\cos(2cQ_z)] \tag{4}$$

for the scattering from a bilayer, *A-B-A* trilayer, and a *A-B-C* trilayer, respectively. The notation {10} indicates an average over the (10), (01), and (11) equivalent reflections. The expressions presented above only consider the scattering due to perfect bilayers and trilayers (i.e., layers in perfect registry with one another). However,

other plausible scenarios of multilayer growth come to mind. One possibility is that as the film thickens the lattice constants vary continuously from layer to layer until the bulk structure forms. Another plausible growth mode might involve a discontinuous change in lattice constants from one strongly influenced by the substrate to one characteristic of the bulk structure. Regardless of the detailed mechanism for multilayer formation, one must also be aware of the fact that as the surface coverage is increased (say, for example, to two nominal layers), the surface film may actually be composed of regions of commensurate bilayer structure separated by domains with slightly different lattice constants, a direct result of the competition of the A-A and A-S interaction energy. Moreover, as the film thickness grows, the possibility that interlayer and intralayer structural reorganization might occur could further complicate a detailed explanation of the microscopic behavior. Inevitably, however, a so-called completely wet solid film must approach a bulklike structure as the coverage is increased. It is with these questions in mind that this work was initiated. A more complete discussion of how one might experimentally test these propositions will be postponed until later in the text.

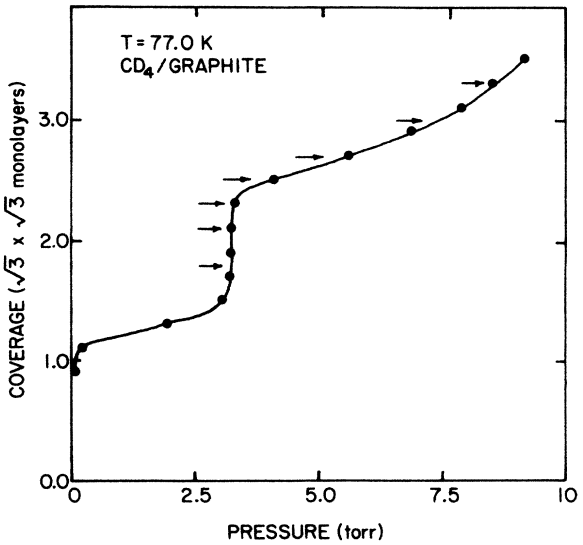

FIG. 3. CD_4 vapor-pressure isotherm ($T = 77.0$ K). The horizontal arrows indicate the appropriate points at which corresponding diffraction data displayed in Figs. 5 and 9 were taken. At coverage $X = 1.0$ the mean surface density is 0.0636 molecules/Å^2.

EXPERIMENTAL DETAILS

The neutron-scattering measurements were performed at the Brookhaven National Laboratory's high-flux beam reactor using a triple-axis spectrometer operated in the elastic mode. The wave number of the incident neutrons was 2.55 Å^{-1}. A bent graphite analyzer crystal was used to select only elastically scattered neutrons. The collimation employed on the spectrometer was 40′ everywhere except in front of the detector which was left open. This resulted in an instrumental resolution of 0.0125 Å^{-1} half width at half maximum (HWHM). Elastically scattered neutrons were collected within the range $1.6 > Q > 2.6$ Å^{-1}. The overlayer diffraction patterns were obtained by subtracting off the background due to the bare graphite. The substrate was a compressed form of vermicular graphite (Union Carbide GTA grade) loaded in an aluminum sample can and mounted on a closed-cycle helium refrigerator. The amount of CD_4 admitted to the cell for the bilayer and trilayer measurements is referenced to the methane vapor-pressure isotherm shown in Fig. 3. During the experimental runs the methane gas (CD_4 research grade) was admitted to the cell at 95 K. It was then warmed to 115 K, and slowly cooled to 50 K over a period of approximately two hours. Further cooling to 25 K was also done at all coverages so as to minimize the Debye-Waller contribution to the scattered intensity. It should be noted that the deuterated form of methane is preferred because of the large coherent neutron-scattering cross section of deuterium. Our attempts to study films which were nominally four layers thick were hampered either by capillary condensation or prohibitively long equilibration times, the latter being more likely the explanation since at no time during these experiments was any evidence of a signal characteristic of bulk methane observed.

EXPERIMENTAL RESULTS

Monolayer

The monolayer regime of CD_4 films on graphite was the focus of several previous studies.[11–16] While preparing to investigate the scattering profiles of bilayer and trilayer CD_4 films we first did a study of the compression of the monolayer film at a fixed surface temperature of 50 K. Figure 4(a) shows a typical profile of the monolayer film. The solid line shows that the data can be satisfactorily described by a powder-averaged Lorentzian with a form factor appropriate for isotropically reorienting CD_4 molecules. The effect that introducing additional CD_4 gas into the cell has on the near-neighbor distance is illustrated in Fig. 4(b). [The units of coverage are such that $X = 1.00$ represents the amount of gas necessary to obtain a completed $\sqrt{3} \times \sqrt{3}$ film (0.0636 molecules/Å^2) as determined from the methane isotherm shown above.] The dashed line in this figure denotes the lattice constant for the $\langle 111 \rangle$ near-neighbor spacing of bulk CD_4 at 50 K. Note that for coverages greater than $X = 1.2$ the film can be compressed more than the bulk.[17] Furthermore, the monolayer lattice compression has a coverage dependence which is qualitatively similar to the change in the vapor pressure as shown in the isotherm for CD_4 shown in Fig. 3. The quality of the fit to the monolayer profiles also provides us with a reliable starting point from which to proceed to the multilayer data (i.e., the molecular form factor, powder averaging, etc., have been properly taken into account in the line-fitting procedure).

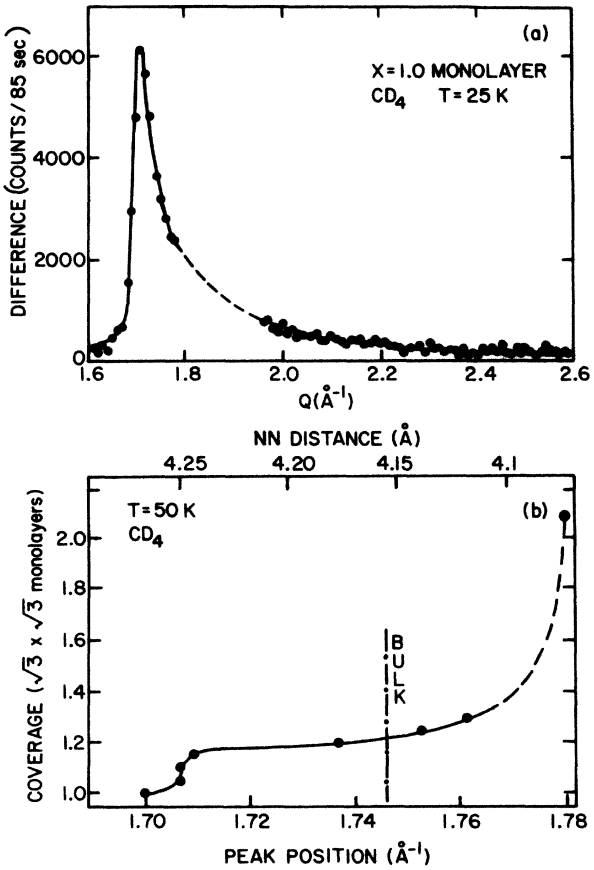

FIG. 4. (a) Typical monolayer diffraction profile from CD_4 at $T=25$ K. Data represent a difference spectrum (i.e., one in which the empty-cell scattering has been subtracted off). The solid line is a powder-averaged line shape described in the text. The dashed line indicates where the scattering due to the graphite (002) peak appears. (b) Plot of methane lattice compression as a function of coverage at $T=50$ K. The dashed vertical marker locates the appropriate near-neighbor distance for the bulk solid.

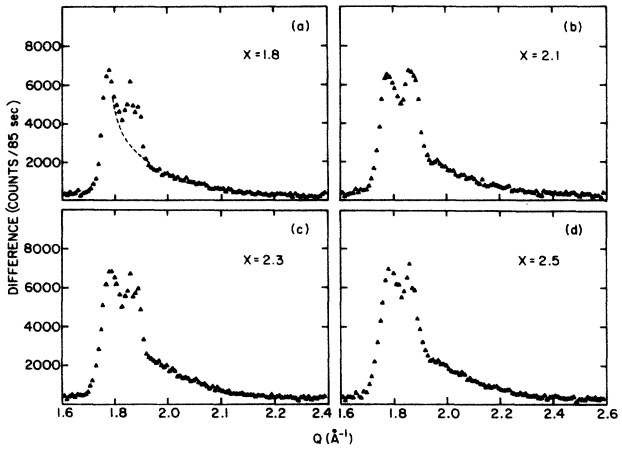

FIG. 5. Diffraction profiles from methane films at $T=25$ K for coverages (a) $X=1.8$, (b) $X=2.1$, (c) $X=2.3$, and (d) $X=2.5$, respectively. The peak at $Q\sim1.84$ Å^{-1} is due to imperfect subtraction of the (002) peak from the graphite substrate; the dashed line in (a) indicates the expected behavior of the 2D diffraction profiles in the region $1.81<Q<1.87$ as described in the text.

Bilayer

Figure 5 displays a series of elastic scans for CD_4 films in the coverage range between $X=1.8$ and 2.5. Although the experimental data exhibit roughly the same scattering profile as was obtained for the model bilayer film in Fig. 2(b), several factors must be kept in mind when trying to fit the bilayer data. As with the monolayer film, the appearance of the graphite (002) peak (which is a direct result of imperfect background subtraction), must be addressed. This can be handled in several ways. By subtracting off an appropriately scaled Gaussian peak with the same HWHM as the experimentally measured graphite peak (taken during the background runs), one can account for most of the excess scattering in this region. Furthermore, we were able to estimate the behavior of the scattered intensity in the neighborhood of the (002) peak by exploiting the shift in the bilayer peak position due to thermal expansion obtained from several scans performed at different temperatures at a fixed coverage. Our subtraction procedure is admittedly not exact, primarily because it neglects the fact that adding layers whose interplanar spacing is different from the graphite substrate not only shifts the position of the (002) peak, but introduces an asymmetry in the diffraction profile directly related to the difference between the interplanar spacing of the adsorbate and the substrate.[18] A problem which is much less easily dealt with is that of accounting for the effect of the thermal motion of the center of mass of the methane molecules, i.e., the familiar Debye-Waller factor. The bilayer line shape exhibits a more gradual trail-off of intensity at large Q when compared to the monolayer case. The Debye-Waller factor, on the other hand, monotonically reduces the scattered intensity with increasing Q. An accurate calculation of the Debye-Waller factor is a nontrivial undertaking for a two-layer CD_4 film, especially at 60 K where anharmonic effects are undoubtably important. We therefore performed the following experimental test. At a fixed coverage of $X=2.5$ a series of elastic scans were made at several fixed temperatures between 20 and 40 K. These scans are shown in Fig. 6. Until the temperature of the system is raised above 30 K, the change in the diffracted profile is clearly negligible. On this basis we conclude that the data taken at 25 K can be properly analyzed by assuming that the Debye-Waller contribution to the scattered intensity is minimal. The most interesting problem encountered in fitting these experimental traces is that the data cannot be satisfactorily fit with either a pure bilayer spectrum or the superposition of two monolayer signals (which might result if the first and second layer lattice constants are not commensurate with one another). Furthermore, the best fit to a perfect bilayer spectrum always required an interlayer spacing greater than 4 Å (a value which is clearly nonphysical). The two-incommensurate-layer fit, on the other hand, did not provide the correct trail-off in intensity at large Q. A much better fit was obtained by assuming that a composite line shape consisting of a com-

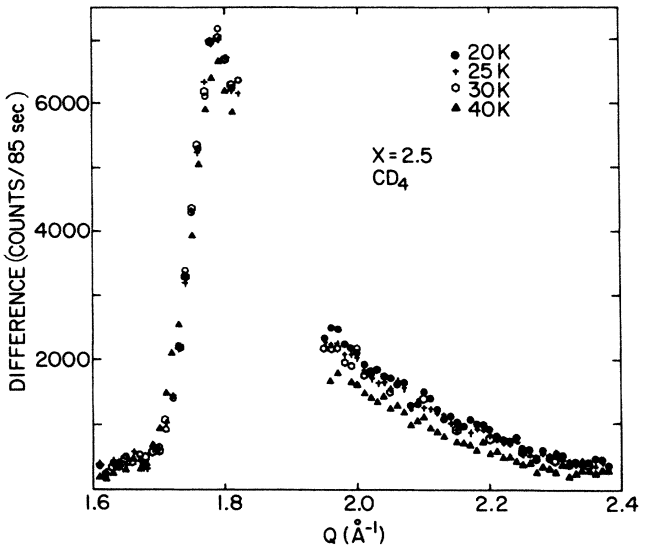

FIG. 6. Temperature dependence of diffraction profile at fixed coverage $X=2.5$. This illustrates that at temperatures below ~ 30 K the thermal contribution to the scattered intensity is minimal.

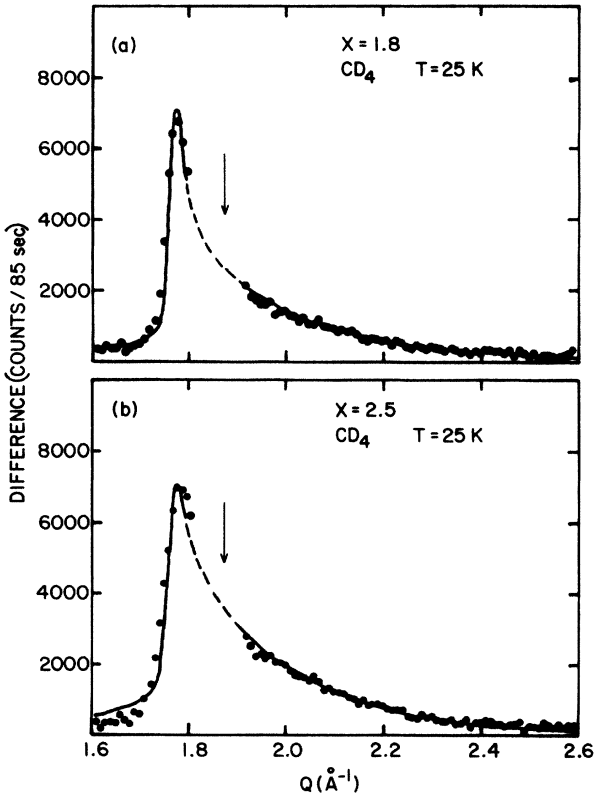

FIG. 7. Typical diffraction profiles and line fits for multilayer data in the region $1.8 < X < 2.5$. The solid-line fit is the result of a composite line shape as discussed in the text. A 0.2 fractional bilayer and 0.8 monolayer component were used in the fit which is shown in (a) whereas for $X=2.5$ in (b) a 0.4 bilayer, 0.6 monolayer composite line was used. The arrows and dashed lines indicate the location of the graphite (002) interference peak. The in-plane lattice constant used for both monolayer and bilayer was 4.10 Å while the interplanar spacing was 3.4 Å. Phillips (Ref. 8) predicts 4.065 Å for the near-neighbor in-plane distance and ~ 3.25 Å for the interplane spacing.

bination of monolayer and bilayer shapes was appropriate. Several such fits using the composite form are shown in Fig. 7. They are, by far, the most satisfactory. As the coverage is increased from $X=1.8$ to 2.5 the fractional contribution to the scattering from the bilayer component is found to increase as would be expected. Furthermore, the total integrated intensity increases linearly with increasing coverage indicating that all the gas molecules contribute to the scattering. The data at $X=1.8$, for example, required a composite line shape with a 0.2 bilayer and a 0.8 monolayer component, while the $X=2.5$ data required a 0.4 bilayer and a 0.6 monolayer component. Figure 8 shows schematically what this might represent in terms of the actual structures of the layers, however, this point will be addressed more explicitly later in the text. The in-plane near-neighbor distance remained fairly constant at approximately 4.1 Å. Since the fits are relatively insensitive to the interplanar spacings the value obtained from the fits to the trilayer data was used.

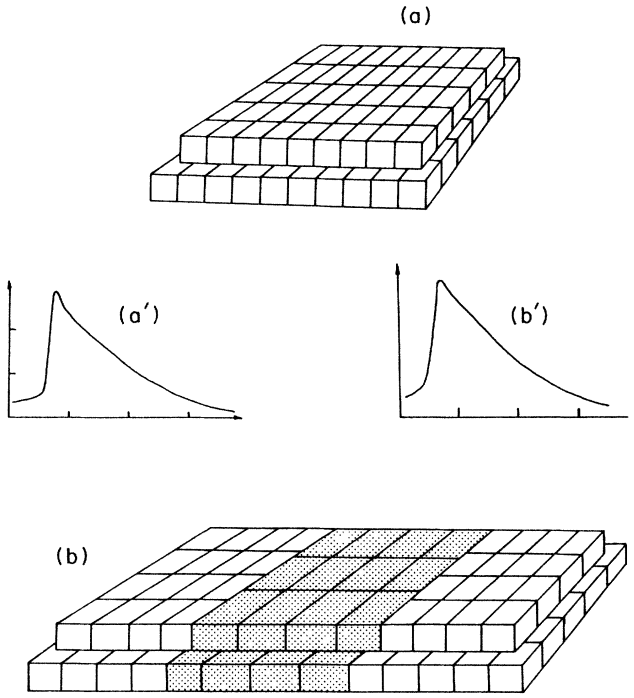

FIG. 8. An exaggerated pictorial representation of two possible ways in which a two layer film could grow. (a) depicts a pure bilayer solid while (b) shows a bilayer composed of regions of high density (unshaded boxes) and low density (shaded boxes). For both cases an *A-B* stacking sequence was used. In (b) the amount of coherent scattering from either structure (unshaded-box or shaded-box region) is less than the fractional amount occupied by either structure relative to the total volume. This is the direct result of the mismatch in the interfacial region and hence adds a monolayer component to the diffraction profile. The appropriate diffraction profile for each structure accompanies each figure and is denoted by the primed symbol.

Trilayer

Figure 9 displays several representative data sets for films in the range of $2.5 < X < 3.3$. Once again we must contend with the imperfect background subtraction of the graphite (002) peak. One can, however, see that by comparing these data with the scattering profiles predicted in Fig. 2 above that the *A-B-C* stacking sequence is the proper choice, consistent with the fcc structure that forms for bulk CD_4.[17] It should also be pointed out that the appearance of the shoulder in Fig. 2(d) above is at the position where the (002) peak for a three-dimensional fcc crystal would appear. The position of this knee in the experimental profiles provides us with at least some idea of the interlayer spacing and helps remove some of the ambiguity in the bilayer data analysis. The behavior of the scattered intensity as a function of temperature at fixed coverage again indicated that no Debye-Waller correction was needed for diffraction scans performed at temperatures below 30 K. Furthermore, fits of the trilayer data to a pure trilayer *A-B-C* spectrum were surprisingly good. The best fit to the data at 3.3 monolayers was obtained using a pure *A-B-C* trilayer line shape and is shown in Fig. 10. The solid line is a fit to the data using the powder-averaged Lorentzian line shape modified to include the structure factor of a trilayer with *A-B-C* stacking. The results are consistent with the lattice constants extrapolated from Baer *et al.*'s data for bulk methane.[17] It is interesting to note that although Phillips assumed in his calculations that the stacking sequence for a three-layer film was *A-B-A* the difference in his results by assuming an *A-B-C* stacking sequence is insignificantly small.[19]

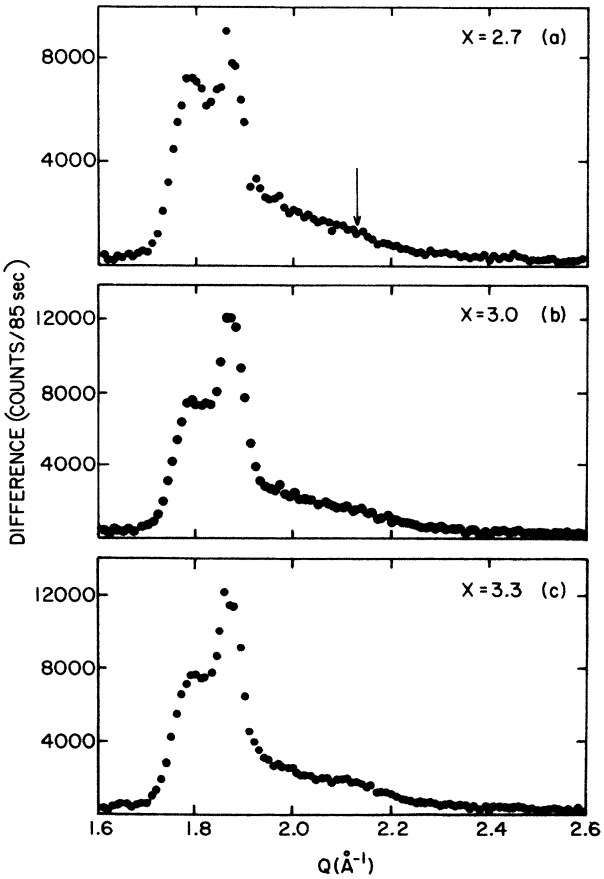

FIG. 9. Diffraction profiles from methane films at 25 K for coverages (a) $X = 2.7$, (b) $X = 3.0$, and (c) $X = 3.3$, respectively. The arrow in (a) indicates the region of enhanced scattering which is the direct resultant of the first appearance of a three-layer *A-B-C* solid contribution to the scattering. The peak at $Q \sim 1.84$ Å^{-1} is due to imperfect subtraction of the (002) peak from the graphite substrate.

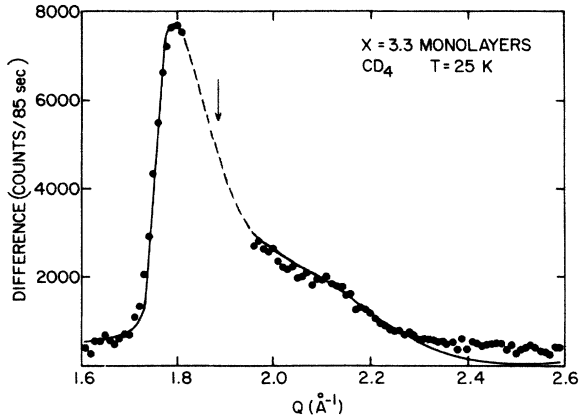

FIG. 10. Diffraction profile at $T = 25$ K for methane coverage of $X = 3.3$. The solid line represents a pure *A-B-C* trilayer fit. The arrow and dashed line show where the graphite (002) interference peak occurs. The in-plane lattice constant used in the fit was 4.15 Å while the interlayer spacing was 3.40 Å. Theoretical predictions by Phillips (Ref. 8) predict 4.04 Å for near-neighbor distance and an interplane spacing of ~3.25 Å. The bulk solid (fcc) has a near-neighbor spacing of 4.16 Å.

The in-plane and interplane lattice constants which gave the fit presented in Fig. 10 were 4.16 and 3.4 Å, respectively. In his model Phillips predicts 4.03 and 3.25 Å for the lattice constants. Our experimental values should allow a refinement of the theoretical predictions. The experimental traces recorded in the coverage regime between $X = 2.7$ and 3.3 could be fit to either a combination of monolayer, bilayer, and trilayer spectra or just a bilayer-trilayer combination (but not uniquely) hence we cannot say more than that either scheme above is consistent with the data.

DISCUSSION

Beginning with the monolayer data, this study has provided some enlightening (and in some ways unexpected) results. First, we find that at 50 K and monolayer coverages greater than approximately 1.25 monolayers the near-neighbor spacing is actually smaller than that of bulk methane at this temperature. For example, at $X = 1.31$ we find a nearly 1% compression with respect to the bulk near-neighbor distance. The diffraction lines in this region ($1.00 < X < 1.35$) remain quite narrow (giving a coherent patch size, $\pi/\Delta_{\mathrm{HWHM}} \approx 250$ Å). At $X = 1.31$, however, there is only a 3% compression of the near-neighbor distance (with respect to the $X = 1.0$ data) for a 30% increase in the total number of molecules on the surface. This indicates that a significant number of

gas molecules ($\sim 21\%$) must already occupy the second layer. Upon increasing the coverage to $X = 1.8$ monolayers we see the first evidence of bilayer solid scattering. The fractional amount of the total scattering due to a perfect bilayer increases progressively rising from 20% at $X = 1.8$ to 40% at $X = 2.5$. These values represent the portion of the composite signal which is due to the pure bilayer. This should not be interpreted to mean that we believe the surface is covered in some regions by a monolayer and the remainder by a bilayer at $X = 2.5$, but instead that a two-layer film covers most of the surface. We imagine this film to be composed of islands of commensurate bilayer surrounded, perhaps, by regions in which a small difference in the near-neighbor spacing between the molecules in the first and second layers exists [i.e., some type of domain wall structure, see Fig. 8(b)]. This may reflect a competition between the *A-A* and *A-S* interactions and the fact that near monolayer completion the film is compressed relative to the bulk value. It may also indicate that some molecules are pinned at the periphery. As the layer thickness increases this mismatch between the natural lattice constant of CD_4 and that imposed by the substrate eventually disappears. Closer examination of the fits to the data in the bilayer region (Fig. 5) reveals that a better fit might be obtained if a monolayer peak with a slightly different lattice constant were also used as a constituent of the composite line shape. This better numerical fit would be a more visually appealing but requires introducing additional fitting parameters, a complication not warranted by the data. We remind the reader that the integrated intensities of the diffraction peaks increase proportionally with the coverage, a fact which demonstrates that all the molecules contribute to the scattering.

A further increase in the coverage (above 2.5) did not, however, lead to a pure bilayer spectrum, but led instead to the first evidence of trilayer solid [see, e.g., Fig. 9(a)]. This was indicated by the distinct increase in the diffracted intensity in the region near $Q = 2.1$ Å which , upon addition of more methane molecules, ultimately develops into the "knee" of the *A-B-C* trilayer spectrum. This behavior suggests that trilayer growth occurs in some regions of the sample even before the bilayer is completed. This fact may not be too surprising from an intuitive standpoint because in this mode of multilayer growth, the $(n+1)$th layer influences the microscopic way in which the nth,$(n-1)$th, . . . layers are formed.[20] Because we are confident that all of the molecules within the cell are diffracting it seems reasonable to suggest that this method of growth is what actually occurs. Furthermore, since the minimum number of layers required for a film which might eventually form a solid with a fcc crystal structure is three, it seems reasonable to suggest that the first evidence of convergence toward bulklike behavior in methane should occur near $X = 3.0$. This might also explain the recent thermal studies of Kim *et al.*[21] in which they used the heat-capacity signal near the bulk orientational ordering transition to study the growth process of multilayer methane. They concluded that methane grows layer by layer for temperatures higher than 25 K. Moreover, they find no heat-capacity anomaly related to the bulk orientational ordering transitions (α-β or β-γ) except for a peculiar broad peak centered at 24.5 K in the range $2.3 < X < 3.9$ registered monolayers (it should be pointed out that in order to convert from our coverage units, registered monolayers, to their coverage units one must multiply the registered-monolayer coverage X by 1.16). Because our highest coverage data indicate that the system appears to be converging toward a structure consistent with the bulk solid it seems reasonable to suggest that the growth mechanism we have outline above could be used to explain the heat-capacity results.

We now address the discrepancy between the theoretical predictions[8] and our experimental findings. The in-plane values for both the bilayer and trilayer films differ by no more than 3.5% from Phillip's predictions. The bilayer in-plane lattice constant is compressed relative to the bulk, in qualitative agreement with theory, whereas the trilayer is slightly more expanded than the bulk, which is contrary to the theoretical model. Although the interplane spacing is predicted by theory to be relatively constant (i.e., temperature independent and roughly thickness independent), we consistently find the best agreement with an interplanar constant which is nominally in the same ratio to the intraplanar constant as would be expected for the (111) stacking sequence of a fcc solid. Intuitively this seems reasonable, although it also seems possible that the interplanar distance could vary as a function of layer distance from the substrate. Because the diffraction profiles were not sensitive to small differences (± 0.1 Å) between interplanar spacings this avenue could not be explored.

SUMMARY

The study of multilayer growth of methane on graphite supports the fact that neutron scattering can be quite useful in learning about the growth mechanism of films on solid surfaces. The data suggest that the films decouple from the substrate in the neighborhood of $X = 3.3$. This point might be experimentally confirmed by attempting to measure the change in surface stress as a function of film thickness.

It seems likely that a study of the multilayer properties of a rare-gas solid should allow a further refinement of this technique and aid in our understanding of such phenomena. The well-established interaction potentials for the nobel gases and the greater number of observable diffracted peaks would also allow a closer comparison between theory and experiment.[20] It is hoped that future studies will be supplemented by incorporating the complementary information contained in the region of the graphite (002) peak. Finally, the possibility of studying the multilayer growth of films on substrates with nontriangular symmetry seems very appealing.[22]

ACKNOWLEDGMENTS

It is with great pleasure that we acknowledge several enlightening and fruitful discussions with J. M. Phillips. We have also benefitted from useful conversations with M. H. W. Chan and P. W. Stephens. Work at

Brookhaven National Laboratory was supported by the Division of Materials Sciences, U.S. Department of Energy, under Contract No. DE-AC02-76CH00016. Work at Northeastern University was partially supported by the Research Corp. and by Northeastern University Research and Development funds. The work at the University of Delaware is supported by National Science Foundation Grant No. DMR8405951. One of us (M.H.) wishes to express his thanks to the U.S.-Japan Cooperative Program for support.

---

*Present address: Institute for Solid State Physics, University of Tokyo.

[1]L. Passell, S. K. Satija, M. Sutton, and J. Suzanne, in *Chemistry and Physics of Solid Surfaces VI,* edited by R. Vanselow (Springer-Verlag, New York, 1986), p. 609 and references therein.

[2]J. G. Dash, Phys. Rev. B **15**, 3136 (1977).

[3]D. E. Sullivan, Phys. Rev. B **20**, 3991 (1979).

[4]R. Pandit, M. Schick, and M. Wortis, Phys. Rev. B **26**, 5112 (1982).

[5]J. Krim, J. M. Gay, J. Suzanne, and E. Lerner, J. Phys. (Paris) **47**, 1757 (1986).

[6]J. J. Hamilton and D. L. Goodstein, Phys. Rev. B **28**, 3838 (1983).

[7]J. M. Phillips and M. D. Hammerbacher, Phys. Rev. B **29**, 5859 (1984); J. M. Phillips, *ibid.* **29**, 5865 (1985).

[8]J. M. Phillips, Phys. Rev. B **34**, 2823 (1986).

[9]P. W. Stephens, P. A. Heiney, R. J. Birgeneau, P. M. Horn, D. E. Moncton, and G. S. Brown, Phys. Rev. B **29**, 3512 (1984).

[10]W. Press, B. Dorner, and G. Will, Phys. Lett. **31A**, 253 (1970); W. Press, J. Chem. Phys. **56**, 2597 (1972).

[11]A. Thomy and X. Duval, J. Chim. Phys. **67**, 286 (1970); *ibid.* **67**, 1101 (1970).

[12]P. Vora, S. K. Sinha, and R. K. Crawford, Phys. Rev. Lett. **43**, 704 (1979).

[13]G. Bromchil, A. Huller, T. Rayment, S. J. Roser, M. V. Smalley, R. K. Thomas, and J. W. White, Philos. Trans. R. Soc. London, Ser. B **290**, 537 (1980).

[14]R. Marx and E. F. Wassermann, Surf. Sci. **117**, 267 (1982).

[15]H. K. Kim and M. H. W. Chan, Phys. Rev. Lett. **53**, 170 (1984).

[16]J. H. Quateman and M. Bretz, Phys. Rev. Lett. **49**, 267 (1982).

[17]D. R. Baer, B. A. Frass, D. H. Riehl, and R. O. Simmons, J. Chem. Phys. **68**, 1411 (1978).

[18]H. Taub, K. Carneiro, J. K. Kjems, L. Passell, and J. P. McTague, Phys. Rev. B **16**, 4551 (1977).

[19]J. M. Phillips (private communication).

[20]W. A. Steele, J. Colloid Interface Sci. **75**, 13 (1980).

[21]H. K. Kim, Ph.D. thesis, Pennsylvania State University, 1985; H. K. Kim, Q. M. Zhang, and M. H. W. Chan, J. Chem. Soc. Faraday Trans. II (to be published).

[22]J. P. Coulomb, K. Madih, B. Croset, and H. J. Lauter, Phys. Rev. Lett. **54**, 1536 (1985).

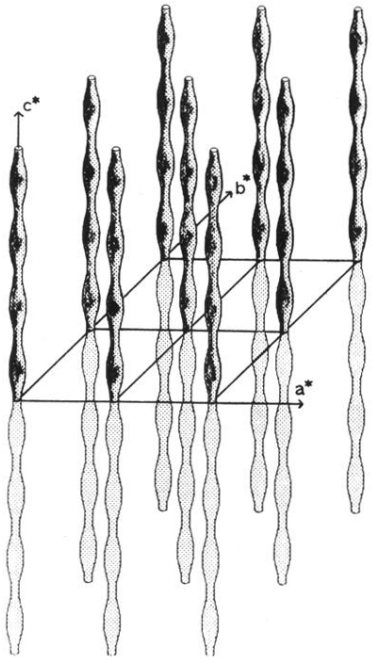

FIG. 1. A schematic representation of a portion of reciprocal space is shown for a spatially finite, bilayer structure.

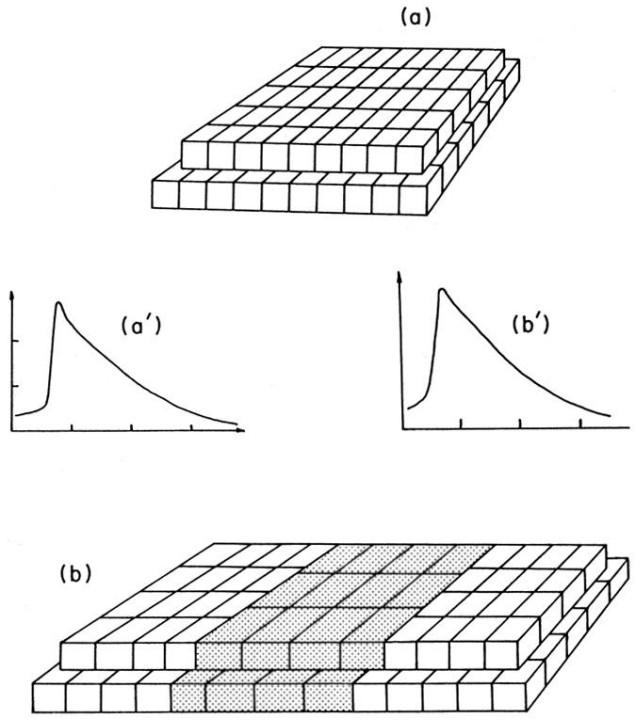

FIG. 8. An exaggerated pictorial representation of two possible ways in which a two layer film could grow. (a) depicts a pure bilayer solid while (b) shows a bilayer composed of regions of high density (unshaded boxes) and low density (shaded boxes). For both cases an *A-B* stacking sequence was used. In (b) the amount of coherent scattering from either structure (unshaded-box or shaded-box region) is less than the fractional amount occupied by either structure relative to the total volume. This is the direct result of the mismatch in the interfacial region and hence adds a monolayer component to the diffraction profile. The appropriate diffraction profile for each structure accompanies each figure and is denoted by the primed symbol.